ORIGINAL RESEARCH   **Open Access**

Assessment of micro-wind turbines performance in the urban environments: an aided methodology through geographical information systems

Antonio Gagliano[*], Francesco Nocera, Francesco Patania and Alfonso Capizzi

Abstract

Among renewable energy sources, the electrical generation from micro-wind turbines has not yet disclosed its huge potential especially in urban settings. Increasing the spread of micro-wind turbines not only promotes the decentralized generation of energy, but also helps tackle fuel poverty and to achieve reductions in the emission of greenhouse gases (GHGs).

This work proposes an innovative methodology to exploit wind flow fields, calculated by means of computational fluid dynamic (CFD) codes in urban environments, within the geographical information system (GIS) platform. In this way, the platform of users is amplified, even non-specialist users, that can utilize wind data to evaluate the potential production of electricity using micro-wind turbines. A pilot study was conducted for assessing the applicability of the approach in a Sicilian city. The results of this case study show the energy yield produced from a building-mounted wind turbine (BUWT). The developed methodology permits to enrich the information usually stored in the GIS platform allowing to supply useful information about suitable sites where micro-wind energy plants can be installed and to assess the production of renewable energy in the urban settings.

Keywords: Renewable energy; Urban environment; Wind turbine; GIS

Background

Power distributed generation is widely seen as a beneficial development in terms of both energy security and decarbonization for the electricity production.

In an urban environment, micro-generation systems [1] represent an opportunity in terms of development for renewable energy sources, research, technological innovation, and resource efficiency. It is current opinion [2,3] that governments' policies should promote the adoption of widespread micro-scale power generation in the urban environments.

Furthermore, the integration of energy and environmental models in urban planning tools is strongly recommended for the development of sustainable communities [4].

In this context, geographical information systems (GISs) are today commonly used in urban and regional scale planning.

The GIS software involves the use of some combination of digital maps and georeferenced data that describe different features of a given area at different scales. It is used for diverse applications: from urban to infrastructure planning, social and economic analysis, and recently also to increase the penetration of renewable energy technologies in urban areas. GIS can support the process of renewable energy source (RES) integration in many ways, such as finding potential areas for solar, biomass, and wind power plants; estimating the RES potential at macro- and micro-scales integrating physical modeling; and analyzing the technical, economic, and social impact of RES projects [5-7].

Therefore, it is interesting to exploit the specific features of the GIS software in order to calculate spatial energy intensity, identify potential sites or land constraints, as well as provide statistical analysis in a straightforward way [8-10].

* Correspondence: agagliano@dii.unict.it
Department of Industrial Engineering, University of Catania, Viale Andrea Doria, 6, 95125 Catania, Italy

The GIS is becoming a very important tool for supporting decision-making in intelligent cities on different sectors. In the era of smart cities, the digital maps and geospatial databases are integrated in workflows in land management, urban planning, and transportation [11].

Currently, micro-wind turbines (WTs) are an emerging technology energy generation in urban area, so there is relatively little empirical knowledge concerning their performance and the corresponding energy yield potential, particularly in the built environment [12,13]. Moreover, micro-WTs with roof-mounting options have recently become available, but their suitability for roof-mounting is still a questionable matter, particularly in urban environments, due to the complexity of the wind distribution [12,14]. One of the barriers for the diffusion of WTs in urban settlements is the difficulty to estimate the wind resource, which is highly site-specific and less predictable than the solar resource. As an example, available wind maps like the 'Wind atlas of Italy' [15] or the Wind Energy Resource Atlas of the United States [16] do not take into account local topographical features such as the presence of buildings, trees, and other obstacles, which cause the variation of wind velocity.

The aim of this paper is to present a GIS-based methodology able to support decision making in energy supply from RESs and energy policies at the urban level. GIS-based planning systems allow planners and citizens to quickly and efficiently create and test alternative energy supply scenarios.

The authors hope that this methodology will be able to support a higher penetration of renewable energy technologies in urban areas.

To achieve this objective, the following steps were implemented: measurement of wind velocity for the site characterization, computational fluid dynamic (CFD) simulation for the calculation of the wind flow within the built area, construction of the digital elevation model (DEM) of the urban area, transferring of wind flow data into the GIS software package.

As a result, local administrations may benefit from an urban wind map in the GIS environment that can be easily consulted, in order to set the wind data necessary for calculating the yearly energy production for a given WT. These issues will be shown in this paper and applied to a pilot study.

Methods
Wind energy
The power generated by a wind turbine can be expressed as [17]

$$P = \frac{1}{2} C_p \rho v^3 f(v), \tag{1}$$

where ρ is the air density, v is the wind speed, $f(v)$ is

the wind speed distribution, C_p is the power coefficient of the rotor. The power coefficient is defined as the ratio between the energy extracted and the wind energy available, and its maximum value is 16/27 (Betz limit). The real C_p is much lower than the Betz limit: especially for micro-WTs, values in the range 0.2 ÷ 0.25 can be assumed. The value of C_p also includes mechanical and electrical losses; thus, the real value is always lower than the theoretical limit.

Wind speed is the most important parameter to be considered when addressing the design and the operation of wind turbines, since its probability density distribution greatly affects the performance. The typical two-parameter Weibull is a flexible distribution that is useful for describing unimodal frequency distributions of wind speeds at many sites [18].

The probability density function of Weibull can be expressed as follows:

$$f(v) = \frac{k}{A} \left(\frac{v}{A}\right)^{k-1} e^{-\left(\frac{v}{A}\right)^k}, \tag{2}$$

where $f(v)$ is the probability of observing a wind speed v, k is the Weibull distribution shape factor, and A is the Weibull distribution scale factor.

The Weibull distribution is important for the assessment of the wind energy potential and wind characteristics; therefore, it is necessary to determine its parameters properly. In this case, the Weibull distribution not only agrees better with wind speed data, but also represents the wind power potential much more accurately.

The two parameters A (m/s) and k (dimensionless) that administer the profile of the Weibull distribution curve are determined from the long term wind data for the candidate site. Higher values of A mean that the distribution is spread over a wider range. On the other hand, if the value of the shape parameter k is between 1 and 2, then the distribution is tilted towards lower wind speeds whereas higher values of k provide a distribution skewed towards higher wind speeds [19-21]. Several techniques can be used to determine the Weibull parameters to fit Weibull distribution to the measured data at a certain location [22,23].

Shape and scale factors can be determined by the mean wind speed standard deviation method using the following equations:

$$k = \left(\frac{\sigma}{V_{\text{av}}}\right)^{-1.086}, \tag{3}$$

$$A = \frac{V_{\text{av}}}{\Gamma(1 + {}^1/_k)}, \tag{4}$$

where Γ is the gamma function, V_{av} is the mean wind speed and σ is the standard deviation calculated by

$$V_{av} = \frac{1}{N}\sum_{i=1}^{N} V_i, \tag{5}$$

$$\sigma = \left[\frac{1}{N-1}\sum_{i=1}^{N}(V_i - V_{av})^2\right], \tag{6}$$

where N is the number of data.

The annual energy can be calculated by multiplying the power output of the wind turbine $P(v)$ for each wind speed for the total number of hours when the velocity v occurs.

$$E_v = 8,760 \sum f(v)P(v) \tag{7}$$

Power curves $P(v)$ depict the relationship between wind speed and power in the range of operation of the turbine. It should be noted that the above equation does not take into account the dynamics of the turbine in responding to rapid changes in wind speed; furthermore, it neglects the effects of rotor dynamics and the various mechanical devices used to avoid overspeeding and the damage of WTs for high wind speeds.

Micro-wind turbines

WTs can be classified into horizontal axis wind turbines (HAWTs) and vertical axis wind turbines (VAWTs). HAWTs are very sensitive to the changes in wind direction and to the turbulence phenomena which cause a negative effect on their energy performance. Rotor needs to be positioned in the wind direction by means of a tail or a yaw motor. Optimum locations for HAWTs are open areas with smooth air flow and few obstacles.

The variation of wind direction has less negative effects for VAWT because they do not need to be positioned into the wind direction. VAWT are usually designed for the deployment in the urban environment. Mertens et al. [24] conclude that certain VAWTs are preferable to HAWTs for roof-mounting upon (high) buildings. VAWTs do not suffer as much from reduced energy outputs, as a result of frequent wind direction changes, whereas HAWTs must yaw and track the wind to be able to extract energy economically.

Although long-term data about the performance of VAWTs are currently not widely available, VAWTs have (in theory) several advantages over HAWTs such as follows:

– Less maintenance as they can operate at lower rotational speed; there is no yawing mechanism to turn the blades towards the wind (fewer and slower moving parts); the generator is often placed under the rotor or on the ground, and so it is easy for repair and maintenance;
– Less aerodynamic noise as they operate at lower tip speeds;
– Turbulence and winds from all directions are handled more effectively, which can be a very important factor for WTs installed in residential area;

Integration of WTs in urban area must be considered from the aesthetic point of view, and all the installed energy systems should be adapted to the building architecture.

Usually, regulations do not permit WTs mounting on roof top of buildings in conservation areas or in world heritage sites [25]. Building-mounted wind turbines (BUWTs) must overcome some fundamental issues that are less binding for other micro-generation technologies, such as mounting method, vibration transmission to building, noise effect, flicker affecting neighbouring houses, shadows and reflections, maintenance access to the turbine, electromagnetic and/or electrical interferences, driver distraction, and so on. In this context, it is useful to report a Summary of Planning Guidelines suggested by the UK Government for the installation of micro-wind turbines [3].

Wind turbines on normal buildings are permitted if

- < 3-m above ridge (including the blade) and diameter of blades < 2 m;
- Internal noise < 30 dB;
- External noise < 40 dB;
- 'Garden' noise < 40 dB;
- Up to four turbines on buildings > 15 m (as with antennas);
- Vibration < 0.5 mm/s.

No roof top-mounted turbines will be allowed on buildings in conservation areas or world heritage sites. Concerning noise pollution, in Italy rules are very strict in the urban environment and set limits for the urban noise, both diurnal and nocturnal, through the equivalent continuous sound level (LAeq). Typically, cumulative turbine noise limits are daytime 55 dB(A) and night time 45 dB(A) [26].

BUWT installations can also perform a complementary function beside photovoltaic (PV) plants considering the seasonal anticorrelation in the time pattern of the wind and solar resources [27].

Computational fluid dynamic

CFD is applied in areas ranging from cooling nuclear reactors to characterization of environmental pollution. In this study, CFD will be used to investigate

wind dynamics around urban areas and to identify sites that have suitable wind energy potential for electric power production. There is a wide range of researches based on numerical simulations using CFD to investigate the natural wind characteristics in urban settings [28-31].

Other studies tackle the influence of various calculation conditions (such as the size of computational domain, grid resolution, boundary conditions, choice of turbulence model, and so on) on the results of CFD simulation [32].

CFD codes solve complete the three-dimensional Navier–Stokes equation for describing the motion of a real fluid. The final expression of the Navier–Stokes equation is originated from the stress–strain relationship of Newtonian fluids:

$$\tau_{ij} = P\delta_{ij} - \mu\left(\frac{\partial v_j}{\partial x_i} + \frac{\partial v_i}{\partial x_j}\right), \tag{8}$$

where

- τ_{ij} is the tensor of the deformations with normal j and direction i;
- P is the pressure;
- δ_{ij} is the Kronecker delta which is zero if $i = j$ and 1 if $i \neq j$; and
- μ is the viscosity.

The term in brackets represents the rate of angular deformation of the fluid. The Navier–Stokes equation is obtained from the motion equation which is given below:

$$\rho\frac{dv_i}{dt} = \rho f_i - \frac{\partial\tau_{ij}}{\partial x_j} \tag{9}$$

where

- ρf_i is the mass forces (gravitational forces) and
- $\frac{\partial\tau_{ij}}{\partial x_j}$ is the term which considers the tensor changes in internal fluid volume.

The Navier–Stokes written in its classical formulation takes the form

$$\rho\frac{dv}{dt} = \rho f - \nabla P + \mu\nabla^2 v, \tag{10}$$

where

- ∇P = pressure forces
- t = time
- v = wind velocity

The Navier–Stokes equation is usually solved numerically because of their non-linearity by using the processing technique called 'at large vortices' (Large Eddy Simulation-LES).

In this study, the 3-D wind flow modeling and visualization software Virtual Wind [33] was used to calculate the wind flow field in the urban area.

The large eddy simulation is solved with the Smagorinski model (sub-grid scale) that uses a second-order scheme for the convective terms in the equations of moment and a second-order centered difference scheme for diffusive terms [34].

The corrector step, which requires the continuity equation, needs the solution of the Poisson equation for pressure. The virtual wind uses a direct FFT method to solve this equation, making this step not iterative. The resolution scheme uses the predictor-corrector method and as corrector uses a Poisson fast Fourier transform solver [35].

Wind flow in the built environment

A crucial factor in the development, siting, and operation of a BUWT is the ability to assess and characterize available wind resources.

Even small reductions of velocities cause significant loss of power, as Equation 1 indicates, so extreme care has to be taken in locating the optimal installation spot for turbines. Wind flow patterns change significantly in any direction in built environment: areas separated by very small distances can be characterized to very different wind speeds. Buildings cause flow separation, which can lead to zones of high turbulence intensity and velocity gradients, which could be problematic for micro-wind turbines. Wind acceleration near the buildings can be exploited to gain advantage for energy generation, e.g. orienting the buildings towards the most common wind directions and/or introducing a sloped side to increase the wind speed. The relative heights and orientations of buildings have also a profound effect on the wind flow. Ledo [36] pointed out that the reasons behind the limited installation of micro-WTs in urban areas are the low wind speeds, high levels of turbulence and relatively high aerodynamic noise levels generated by the turbines. Blackmore [37] and Rafailidis [38], asserted that one of the main factors affecting the performance of roof-mounted wind turbines is the building roof shape (roof effect). Other studies investigated the mounting location and analyzed the flow around pitched, pyramidal, flat, and gabled roofs with a view to developing small wind turbine sitting guidelines focusing on the mounting height [36,39,40].

The disturbed flow zones must be identified and avoided when choosing the site of installation of BUWTs. Local direction, speed, and wind turbulence depend on the shapes of buildings [41].

Wind potential in urban areas can essentially be determined in three different ways [42]:

– *In situ* measurements at least over a 1-year period directly at specific sites;
– Wind tunnel experimental tests;
– CFD calculations.

In situ measurements are probably the most accurate tool for assessing wind flow in a specific site, especially in the case of energy retrofitting of existing buildings for which the use of BUWTs is foreseen. However, this approach requires months or years of data acquisition, and the major drawback of this method is the high cost.

On the other hand, wind tunnel tests require the construction of an accurate physical model of the area around the buildings and the collection of distribution data of wind speed. This approach is slightly faster but also significantly more expensive. In addition, it is difficult to accurately model the effect of turbulence in a wind tunnel because it is limited by its size, and the results could be affected by significant errors.

On the contrary, the CFD approach is a practical and effective alternative to the other two approaches. CFD commercial packages have gained a good credit both in research and academic communities as well as in engineering consulting societies, thanks to their capability of providing an insight into the flow field around the buildings. Moreover, the first two approaches determine the wind velocities only in few points at the same time; instead, the CFD analysis allows to calculate the flow field within the whole investigated area. Thereby, the CFD simulations, in conjunction with a detailed model of the urban environment, allow to simulate the wind flow field around the buildings where the BUWTs could be installed. The CFD simulations do not provide information about wind intermittency, transients, etc.

Overall, it is very hard to predict wind speed in a specific site within the built-up areas. However, some general patterns can be identified to ensure the placement of the turbine into the undisturbed region, outside of the areas of turbulence:

– WTs should be positioned near the center of the roof where the wind is stronger;
– WTs should be positioned so as to meet the most frequent wind direction;
– The mast of the turbine should be approximately 50% taller than the surrounding objects;
– The lowest position of the rotor has to be at least 30% of the building height above the roof.

The wind flow field in the urban area is still extremely difficult to predict even for simple surrounding environments. Nevertheless, despite the widespread use of CDF simulations, the prediction accuracy and many factors that might affect simulation results are not yet thoroughly understood [43].

The GIS-based methodology

In this paper, a GIS-based methodology was developed as useful support to improve the diffusion of micro-wind turbines in urban environment. The proposed methodology needs the knowledge of several data, requires the use of different software as well as their reciprocal integration. The general pattern is depicted in the following:

Wind site characterization

The assessment of the production capacity of specific WTs, as well as the evaluation of the related technical and economic issues, requires data regarding wind speed and direction of a certain statistical significance acquired through systematic recordings over a period of 1 year or more. The analysis has to provide an estimation of the marginal distribution of wind intensity and direction and the Weibull statistical distribution.

Wind climatology characterization has to be developed starting from available anemometric data.

GIS mapping

The three-dimensional (3D) digital models, normally used for GIS applications, use square mesh (DEM or DTM) or triangular mesh. The triangular irregular network (TIN) is a vector-based representation (a digital data structure) used for the representation of a surface made up of irregularly distributed nodes and lines with three-dimensional coordinates (x, y, and z) that are arranged in a network of non-overlapping triangles. An advantage of using a TIN over a raster DEM in mapping and analysis is that the points of a TIN are distributed variably, based on an algorithm that determines which points are most necessary to an accurate representation of the terrain. ArcGIS uses Delaunay's triangulation method [44] to construct these triangles. On the other hand, TIN meshes are appropriate for contexts where morphology is gentle and continuous without sudden changes of height above the ground, but they do not supply a good representation of complex morphology that is characteristic of urban areas (presence of buildings). Therefore, a TIN-modified model suitable for urban environment was developed considering the terrain map and also the building elevation [8]. The ESRI software ArcGIS Desktop v.9.2 with Spatial Analyst and 3D Analyst extensions was used [45].

Interface between CFD and GIS

A crucial point of the procedure is the process of interface between the output files of the CFD simulations

and the GIS environment: interaction between the CFD code and the GIS software is essential. The output files of CFD simulation are 'raster' files which contain the information on the values of wind velocity; wind velocities are represented with square-colored pixels in accordance with a default scale. The GIS software is not able to directly read these files, so it is necessary to modify them from RGB images (bands of color: red, green, blue) into gray scale images as shown in Figure 1.

After this preliminary operation, the following procedure has to be developed in the GIS environment:

- The CFD files have to be geo-referenced using the specific procedure that manages geographic data. Subsequently, to the process of geo-referencing, new raster files are generated; therefore, geometrical data are stored within a regular matrix (GRID) organized as a set of rows and columns. The size of the cells establishes the level of spatial resolution. Each cell of the GRID contains its own height above ground level (GRID-quote) and a set of 'information' that can be a particular geographic feature or other data, such as the wind speed. Then, the raster dataset can be displayed or rendered in many different ways.
- The 'stretched renderer' procedure displays the continuous raster cell values across a gradual ramp of colors. The stretched renderer works well when a large range of values is displayed such as in spectral imagery, aerial photographs, or elevation models. In this way, the gray scale, which represents the field of wind velocity (CFD output file), is archive, defining a rule to describe the variation of velocity into a value of velocity at each cell. Choosing a linear variation for the velocity implies that the black color is associated to the minimum value of velocity and the white color is associated to the maximum value of velocity. The results of these operations are raster

files which provide for each cell the value of wind velocity calculated through CFD simulations.
- Additional raster files can be generated using the function 'Raster Calculator' of the plugin 'Spatial Analyst' of ArcGIS® [45], which permits to execute mathematical operations using the data contained in two or more raster files. Therefore, it is possible to create new raster files, which give for example the average value of the wind speeds calculated by means of the CFD simulations considering different wind directions.

In conclusion, the proposed procedure generates raster files which contain the wind speed at each point P (x, y, z) of the investigated urban area. Figure 2 shows the render of a raster file which provides the wind flow field within the built-up area.

CFD simulations
The Virtual Wind software was used to calculate the whole flow field in the investigated urban area. The choice to use a simple CFD code, like the Virtual Wind which is not intended for high-end CFD analysis, has the aim to allow, also for users who are not specialists, a quick prediction and comprehension of wind flows in complex environments.

The Virtual Wind needs to be supplied with predefined terrain geometry, which must obey a limited set of restrictions (i.e., the border of geometry to be recognized, as terrain cannot overlap itself). Virtual Wind works when connected as a plugin to Google Sketch up; thereby, it is quite simple to model the built up area.

Sáenz-Díez Muro et al. [41] used the Virtual Wind code to optimize the implementation of mini wind turbine in the urban environment.

Moreover, this CFD code was used as an internal analysis tool within its parent company, RWDI, for
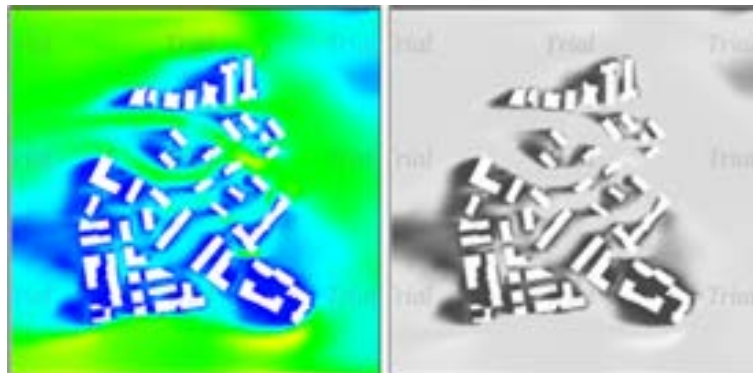

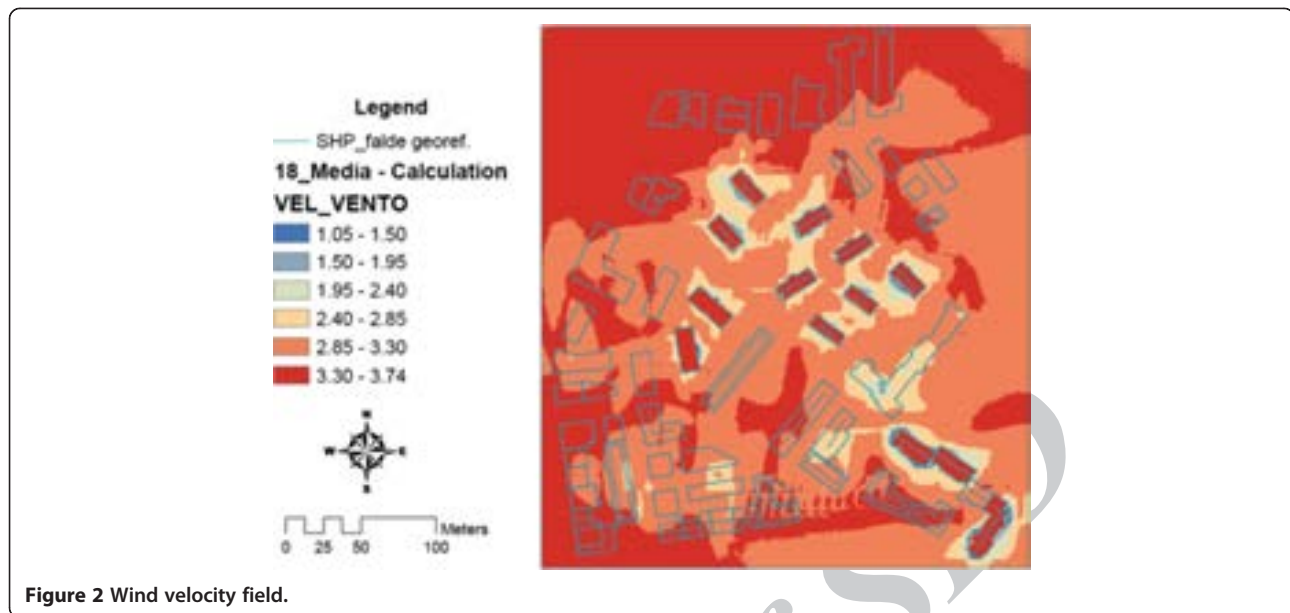**Figure 1 Example of transformation from RGB to grayscale image.**

Figure 2 Wind velocity field.

approximately 5 years before it was released commercially. It has been run on hundreds of internal projects [46].

BUWTs energy production

The above procedure provides the average wind velocity in each point of the built-up area. Therefore, it is possible to calculate, once the parameters of the Weibull distribution are defined, the wind velocity distribution by Equation 2. Hence, the yearly energy production of a BUWT is calculated by Equation 7.

Comprehensively, a methodology has been developed that can provide a very detailed information about the wind velocity in urban areas.

A fundamental feature of the methodology is its high geometrical resolution; indeed, a spatial resolution of 1.0 m × 1.0 m is adopted, which is far more accurate than other wind atlases, based on air flow models that account for the effects of topography using an horizontal scale of 1 km^2 (e.g., NOABL 2012) [47].

Pilot study

The proposed methodology was tested and verified by means of a first pilot study. In the following, the authors will report the results obtained for an urban area of the municipality of San Cataldo, a city located in the centre of Sicily (latitude: 37°29′0″N, longitude: 13°59′0″E). The wind data were provided by two weather stations installed within an urban area of San Cataldo, for a period of about 3 years. These weather stations provide both speed and wind direction, measured by means of anemometers at 20.0 m above ground. The wind rose gives the following information:

– The wind velocity has not prevailing directions;
– The investigated urban area has a weak wind potential.

The above-mentioned wind measurements were used to calculate the average wind speed (V_{av}) along the four cardinal directions (Table 1).

The lowest mean wind speed (2.20 m/s) was measured in the North sector; in the East, West, and South sectors, the mean wind speeds are quite similar between them, and they are all below 3.0 m/s. Amongst the most important recorded anemological data, the frequency distribution of wind speed is of specific interest.

According to the measurements of wind speed, it is necessary to use estimation methods to derive the parameters k and A on the basis of available data of the mean wind velocity V_{av}. Considering the peculiarity of the built-up areas, three Weibull probability functions were compared, which used the same value of shape factor (k) = 1.4, and three different values of the distribution scale factor (A): A_1 = 2.085, A_2 = 1.5 V_{av}, and A_3 = 6.0.

The above values were chosen in agreement with literature data [12]. Figure 3 shows the wind speed frequency

Table 1 Yearly average wind speed

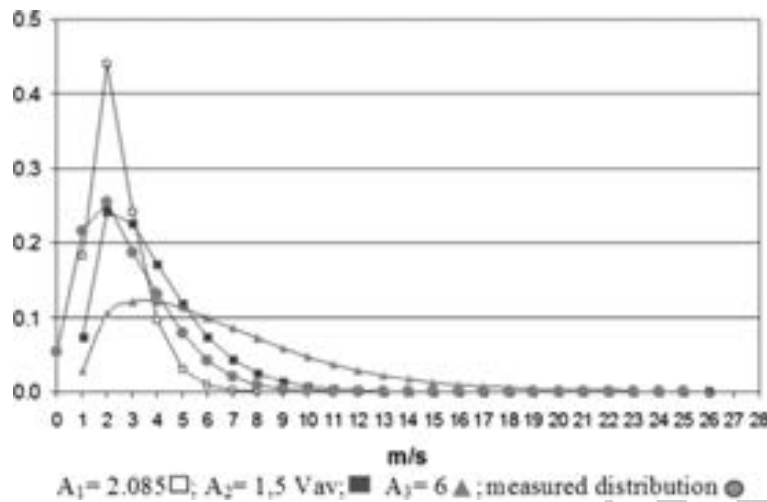| Direction	North	West	South	East
Mean velocity V_{av} (m/s)	2.20	2.88	2.91	2.71

Figure 3 Measured and Weibull wind frequencies.

obtained both by measured data and by Weibull frequency distributions.

It can be noticed that

– The Weibull frequency distribution obtained, adopting the scale factor $A = 1.5\ V_{av}$, is the one which approaches better the measured wind frequencies; and
– Wind speed frequency is high around $2.0 \div 3.0$ m/s, while low frequencies occur for speed above 7.0 m/s.

Results and discussion

CFD simulations require as input both wind data and the model of the geometry of the built-up area. The 3D models of the terrain, including the buildings, were created through Google Sketchup, a widespread CAD tool used for creating built-up area. Therefore, the 3D model of the terrain is easily imported in Virtual Wind as a plugin. The supply input parameters for the simulations were wind speed, simulation resolution, spatial extents, and monitored quantities. The size of the calculation domain is $x = 325$ m, $y = 360$ m, $z = 30$ m. Uniform computational grid was adopted across the whole calculation domain. Thermal stratification and density variations were not considered.

Figure 4 shows the 3D modelization of the investigated area.

To accurately simulate wind flow in the built environment, velocity profiles at the inlet boundary surface of the calculation domain must be accurately modelled.
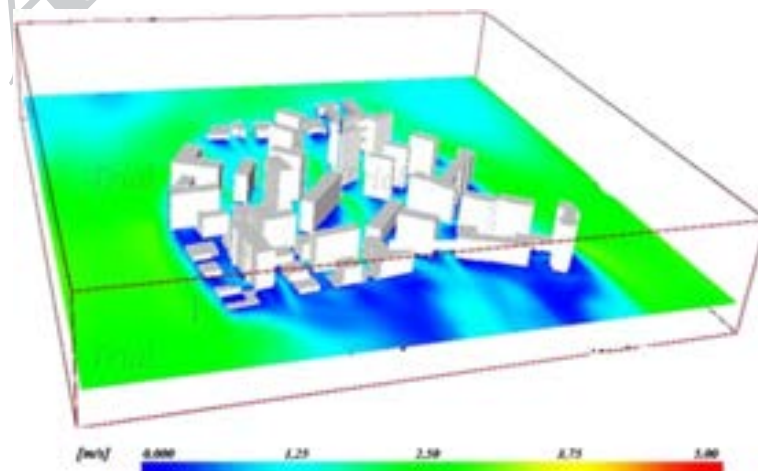

Figure 4 3D view of the calculation domain.

The vertical profile of wind velocity was calculated as a function of the roughness of the ground:

$$V_2 = V_1(h_2/h_1)^{\alpha}, \tag{11}$$

where V_2 is the wind speed at the height h_2, V_1 is wind speed at the original height h_1, and α is the surface roughness coefficient, assumed to be 0.28. It has been underlined that the power law profile with an exponent $\alpha = 0.28$ overestimates the velocity profile below the mean building height, while it underestimates the profile above the building [48]. CFD simulations provide the wind flow field, on the XY plane at whatever heights above ground level (AGL); thereby, it is possible to detect the most suitable locations for turbine mounting. Figure 5 shows the wind flow field in the case of wind blowing from West direction and $h = 6.0$ m. To investigate the effect of wind direction, simulations were run with different wind directions (North, East, South, and West).

The analysis of the wind flow field indicates that large streets with an aspect ratio $d/h > 1.5$ (d = street width, h = building height) are characterized by higher wind speeds, up to 3.45 m/s, and consequently, these zones could be the most suitable for the installation of micro-wind turbines integrated into the poles of public illumination.

Mounting small wind turbine systems to the corner or the side of a building may take advantage of the favorable flow between buildings.

On the contrary, narrow streets with an aspect ratio $d/h < 1.5$ are characterized by lower wind speeds. Figure 6 shows the wind flow field on a vertical plane.

It is possible to notice that the wind field is affected by the shape, height, and relationships that buildings have with each other and to visualize an effect of disturbance generated by the taller building and the extension of the disturbed area. Furthermore, it is possible to highlight the zones where there is a significant reduction of wind speed (blue color) and the zones where the wind speed is stronger (green or yellow color).

The analysis of the vertical profile of the wind velocity at the point 1 in Figure 7 was also performed, placed near a building 23.0-m tall.

It is possible to observe the abrupt reduction of the wind velocity in correspondence of the height of the adjacent building and the increase of the velocity above the height of 26.0 m, that is out of the disturbed zone.

With the aim to validate the numerical results of CFD simulations, a comparison with other researches and literature data were performed for similar geometries [49,50]. Such analysis indicates a good correlation and agreement between our results and bibliographic data. Moreover, the calculated values of wind velocity were compared with experimental measurements in two points (anemometric stations), observing differences in the order of 10 ÷ 15%. Obviously, a more extensive campaign of experimental measurements could further confirm the reliability of this study.
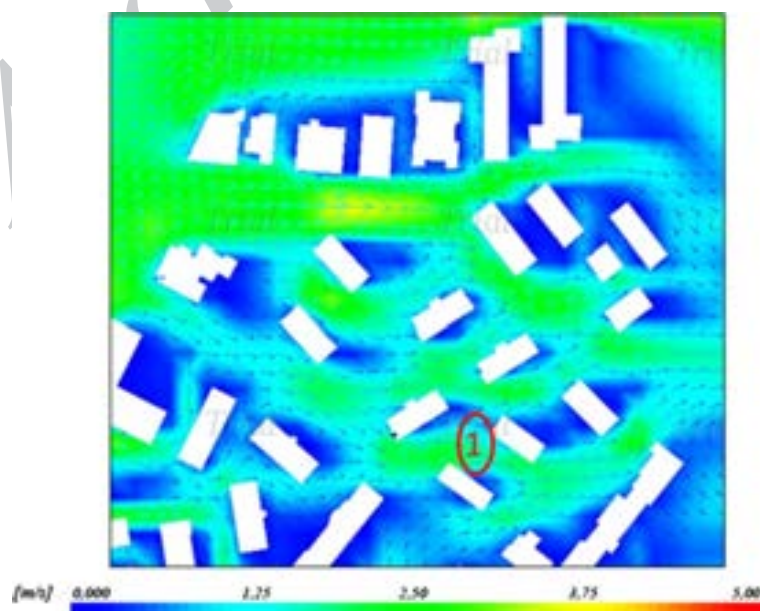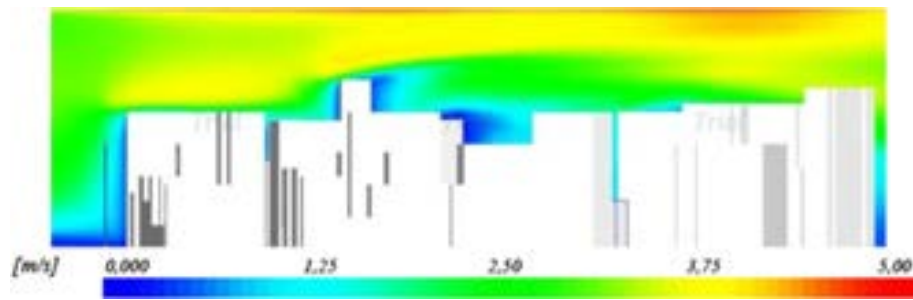

Figure 5 Wind flow field at a horizontal plane.

Figure 6 Wind flow field on vertical plane.

GIS mapping

The digital elevation model of the urban area was built using data carried out from large scale vector mapping (scale 1:2,000) that provides both the data of the morphology of the terrain and the data related to the anthropic elements (buildings, plants, vegetation, and so on). Otherwise, in the 'classical' approach, which represents each building with a single polygon which is the gutter surface of the building, the adopted model introduces a second polygon, placed very close to the ground surface. This second polygon acts as a 'break line' in the 3D modelling. It is 'shrinked' with an offset of 5.0 cm from the polygon which represents the building, and it allows to differentiate the buildings and the ground surface. This strategy has the advantage to create a very reliable and well representative TIN of the built-up area (Figure 8).

The accuracy of the raster data is strongly related to the GRID resolution where these data are recorded. In this study, the GRID is characterized by a size mesh of 1.0 m × 1.0 m in the *XY* plane. Therefore, each cell of the GRID contains the information concerning its own quote (GRID-quote).

Wind mapping

As previously discussed, a nodal point of the proposed methodology is the possibility to interface the output of CFD simulations with the GIS environment. Adopting the above illustrated procedure, it was possible to obtain at any spatial position of the built-up area, the mean wind velocity calculated by means of the CFD simulations. The overall result of the study is the possibility to generate the wind maps for any height AGL. Figure 9 shows the average wind velocity as stored into the GIS software.

Wind maps were elaborated for different heights AGL: 9.0, 18.0, and 24.0 m. The height of 9.0 m was considered as representative of BUWTs mounted on the poles for public lighting; instead, the heights of 18.0 and 24.0 m were considered as representative of BUWTs mounted on the roof of the buildings.

Wind maps, customized in the GIS software, supply the average wind speed and the needed parameters to define the wind velocity distribution (Weibull distribution), which are the most important data necessary to calculate the power output of BUWTs in a realistic way. Thereby, inhabitants of the district can use this tool to calculate the yearly energy obtainable by WTs in every point of the urban area.

The aesthetics of BUWTs has to be complementary rather than in contrast with the nearby buildings to ensure their acceptance in the urban context.

Figure 10 shows an example of aesthetic integration of BUWT pole mounted in the building environment of San Cataldo city.

In any case, both the visual and noise impacts of micro-wind turbines should be assessed by the Local Planning Authority.
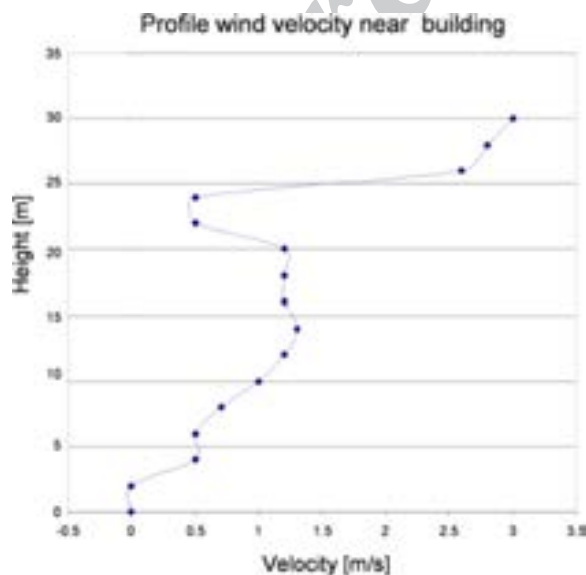

Figure 7 Vertical wind shear (point 1 in Figure 5).

Figure 8 Overlapping between DEM model and ortho-photos.

Annual energy production

The above procedure allows to import the wind maps for the investigated area in the GIS platform. Starting from that, a comprehensive analysis of the energy performances of three commercial models of BUWTs are developed. Power curves and main technical specifications of the selected WTs are reported in Table 2 and Figure 11.

As previously mentioned, within the investigated area, two alternatives for mounting the BUWTs were evaluated:

a) On the pole of public lighting ($h = 8.0$ m), where the average wind speed of 3.50 m/s was obtained consulting the GIS database; and

b) On the roof of buildings ($h = 24.0$ m), where the average wind speed of 4.80 m/s is available according to the GIS database.

The yearly energy production was calculated by Equation 3 as a function of the wind velocity distribution and the BUWTs manufacture power curves.

Table 3 shows the year-round performance of the three micro-wind turbine. It was assumed that positive energy output starts immediately when the wind meets the cut-in speed.

One can observe the following:

- A turbine mounted on the roof of the building takes advantage of the building height; therefore, the
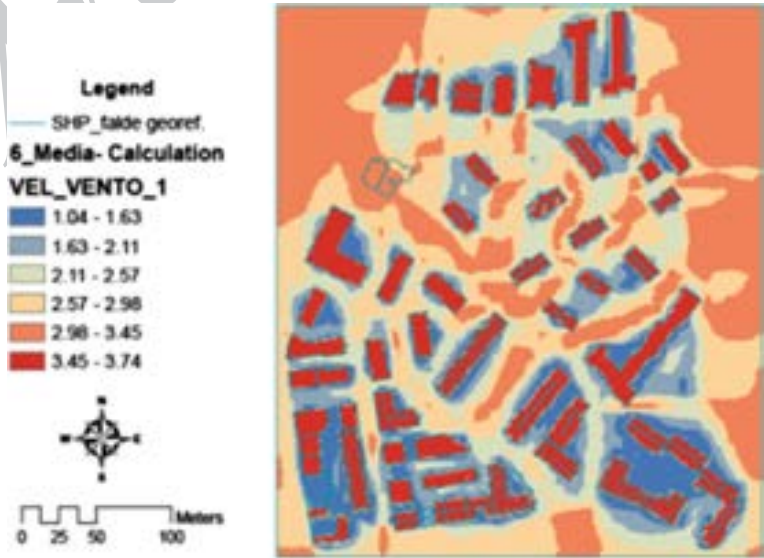

Figure 9 Average wind velocity at 6 m (AGL).

Figure 10 Photo-simulation of WT urban integration.

energy production is about 30% higher than for the pole mounting;

- UWT$_1$ and UWT$_2$ (VAWT) give more or less the same annual energy, with a difference of about 10%;
- UWT$_3$ that is a HAWT has the lowest annual energy production, and this is mainly due to its power curve that has poor performance for weak wind velocity. Furthermore, this WT has very large dimensions that are not always compatible for building mounting.

On the whole, the procedure allows to calculate the annual energy for each kind of WT. It is also possible to compare the performance of several WT and consequently to choose the most adequate for the installation in the specific site. The GIS platform also allows to provide for each building other information, i.e., the number of dwellers, the consumption of electric energy (daily, monthly, yearly), and so on. Such information can be useful to evaluate statistical match between demand and supply, which determines how much electricity will be exported, as well as for planning the installation of RES.

Economic and environmental benefits
An accurate economic analysis of micro-generation technologies is important as it allows prospective buyers to assess the financial outlay and the annual and total payback period of the turbine. The electricity generated by the BUWTs means direct savings for the owners through a lower electricity consumption bill, and if the

BUWTs are eligible for feed-in tariff (FiT), it is also possible to earn an added export tariff.

In Italy, wind power plants with a nominal peak power up to 200 kW (micro-generation) can benefit from the all-inclusive tariff grant [51] and thereby receive the incentive of 30€ cents/kWh for 15 years. After the period of 15 years, the energy produced through BUWT will be traded to the national grid. The analysis of the economic viability was performed considering an energy production of 1,468.00 kWh, as reported in Table 3.

The following assumptions were fixed:

- The total cost of the system is 6,000.00€ (4,000.00€ WT + 2.000 for installation, electric connection) [52,53];
- The FiT is 0.30€ /kWh, within the first 15 years [51]; and
- The price is 0.09€/kWh for the following period [51].

The financial analysis indicates a payback time of 14 years which is lower than their estimated life-span of 20 years. The economic feasibility and the market potential for BUWTs is highly influenced by the reduction of WTs costs due to technical progress and by incentive policy. Electricity generated by BUWTs results also in a

Table 2 Technical specifications of micro-turbines

Turbine model	Rated power (kW)	Rated wind speed (m/s)	Cut-in speed (m/s)	Cut-out speed (m/s)	Tower blade height (m)	Typology of WT
WT$_1$	1.5	14.0	4.0	20.0	2.5	Darrieus
WT$_2$	1.5	15.0	3.0	21.0	4.0	Savonius
WT$_3$	2.3	22.0	4.5	22.5	9.0	Horizontal axis
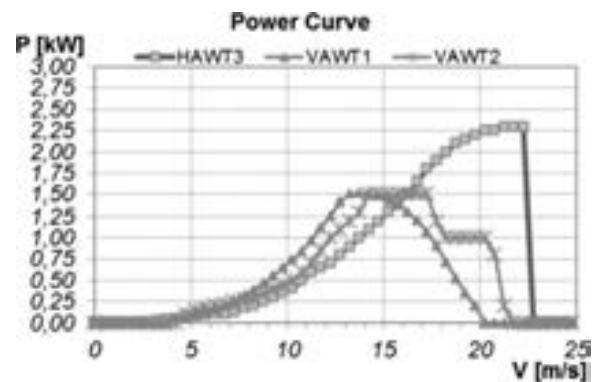
Figure 11 Power curves of selected WTs.

Table 3 Yearly energy production

	Yearly energy production (kWh/year)	
	Pole mounting	Building mounting
$BUWT_1$	628.0	1,468.0
$BUWT_2$	553.0	1,280.0
$BUWT_3$	393.0	910.0

reduction in the emission of greenhouse and acid gases. Carbon intensity of electricity varies greatly depending on fuel source; considering the carbon intensity of network electricity to be 0.527 kg CO_2/kWh [54], it was possible to calculate the ratio between cost investment and emission savings, which is 6.12€/kg CO_2.

Obviously, it is possible to obtain more seductive results with higher average wind velocity, or if more efficient wind turbines will be available on the market. The financial analysis indicates that micro-wind turbines are economically viable also in the built-up area and they can play a primary role in future urban energy supply, such as the PV plants which are widely diffuse in the building environment.

BUWTs should be capable of producing a significant proportion of the annual electricity demand; otherwise, they may become a primary aesthetic feature which would be unsatisfactory from both an environmental viewpoint and that of clients, planners, designers, occupants, and local inhabitants.

Considering that the average Italian domestic household consumes (excluding thermal uses) approximately 3,000÷4,000 kWh per year [55,56], the installation of just one BUWT can cover more or less 40% of the annual energy demand of a single domestic household. Thereby, to increase the capacity credit, that expresses how much 'conventional' power can be avoided or replaced by wind power [57,58], it is useful to install multiple WTs on multi-storey buildings.

Conclusions

The work provides a first step for assessing the feasibility of building integrated wind turbines, encouraging the incorporation of renewable energy sources in new and refurbished buildings, and promoting the adoption of micro-scale power generation in urban environments.

The developed methodology allows creating a useful database in the GIS platform that provides the wind distribution within an urban area by enabling fast and accurate spatial information for calculating the yearly energy production obtainable of micro-wind devices. In this way, owners/occupiers have the possibility to evaluate the effective potentiality of wind energy generation in urban areas.

An innovative aspect of this approach is mainly linked to its high productivity, which allows to automatically extend the evaluation of the potential production from a single site of specific interest to an entire urban area.

Moreover, the integration between GIS software and methodologies to assess potentiality of RES can be a useful tool to support energy conservation programs, planning of local RES energy resources, and implementation of energy strategies as combining micro-cogeneration and poly-generation.

Overall, the research can contribute to the diversification of energy sources and maximization of on-site RES penetration in urban areas in accordance with the objectives set by the EU.

Future developments of the research will be the comparison between the hourly household energy load and the hourly power provided by the BUWTs, with the aim to support the strategies for the dispatch and control of energy in a smart grid with stronger connection between energy demand and supply.

References
1. Bergman, N, Eyre, N: What role for microgeneration in a shift to a low carbon domestic energy sector in the UK? Energy Efficiency **4**, 335–353 (2011)
2. Bahaj, AS, Myers, L, James, PAB: Urban energy generation: influence of micro-wind turbine output on electricity consumption in buildings. Energy Buildings **39**, 154–165 (2007)
3. Peacock, AD, Jenkins, D, Ahadzi, M, Berry, A, Turan, S: Micro wind turbines in the UK domestic sector. Energy Buildings **40**, 1324–1333 (2008)
4. Medrano, M, Brouwer, J, Carreras-Sospedra, M, Rodriguez, MA, Dabdub Samuelsen, G: A methodology for developing distributed generation scenarios in urban areas using geographical information systems. Int. J. Energy Technol. Policy **6**, 413–434 (2008)
5. Voivontas, D, Assimacopoulos, D, Mourelatos, A, Corominas, J: Evaluation of renewable energy potential using a GIS decision support system. Renew. Energy **13**, 333–344 (1998)
6. Byrne, J, Zhou, A, Shen, B, Hughes, K: Evaluating the potential of small-scale renewable energy options to meet rural livelihoods needs: A GIS- and lifecycle cost-based assessment of Western China's options. Energy Policy **35**, 4391–4401 (2007)
7. Caiaffa, E, Marucci, A, Pollino, M: Study of sustainability of renewable energy sources through GIS analysis techniques. Comput. Sci. **7334**, 532–547 (2012)
8. Gagliano, A, Patania, F, Nocera, F, Capizzi, A, Galesi, A: A proposed methodology for estimating the performance of small wind turbines in urban areas. In: Smart Innovation, Systems and Technologies, 12th edn, pp. 539–548. Springer, Heildeberg (2012)
9. Gagliano, A, Patania, F, Nocera, F, Capizzi, A, Galesi, A: GIS-based decision support for solar photovoltaic planning in urban environment. In: Smart Innovation, Systems and Technologies, vol. 22, pp. 865–874. Springer, Heildeberg (2013)

10. Caputo, P, Costa, G, Ferrari, S: A supporting method for defining energy strategies in the building sector at urban scale. Energy Policy **55**, 261–270 (2013)

11. Verma, S: GIS-driven renewable energy framework for smart and sustainable cities. India Geospatial Digest (2013)

12. Allen, SR, Hammond, GP, McManus, MC: Prospects for and barriers to domestic micro-generation: a United Kingdom perspective. Energy **85**, 528–544 (2008)

13. Acosta, JL, Combe, J, Djoki´c, SZ, Hernando-Gil, I: Performance assessment of micro and small-scale wind turbines in urban areas. EEE Syst. J. **6**, 152–162 (2012)

14. Bussel, GJW, Mertens, SM: Small wind turbines for the built environment. In: Proceedings of the 4th European and Asian Wind Engineering Conference, Prague, 11–15 July 2005

15. RSE: Atlante Eolico Interattivo. http://atlanteeolico.rse-web.it/viewer.htm. Accessed 10 May 2013

16. NREL: Dynamic maps, GIS data, & analysis tools. http://www.nrel.gov/gis/wind.html. Accessed 10 May 2013

17. Burton, T, Sharpe, D, Jenkins, N, Bossanyi, E: Wind energy handbook. Wiley, New York (2001)

18. Carta, JA, Ramirez, P: Analysis of two-component mixture Weibull statistics for estimation of wind speed distributions. Renew. Energy **32**, 518–531 (2007)

19. Bhattacharya, P, Bhattacharjee, R: A study on Weibull distribution for estimating the parameters. J. Appl. Quant. Method **5**, 234–241 (2010)

20. Akdag, SA, Bagiorgas, HS, Mihalakakou, G: Use of two-component Weibull mixtures in the analysis of wind speed in the Eastern Mediterranean. Applied Energy **87**, 2566–2573 (2010)

21. Oyedepo, SO, Adaramola, MS, Paul, SS: Analysis of wind speed data and wind energy potential in three selected locations in south-east Nigeria. Int. J. Energy and Environ. Eng. **3**, 1–11 (2012)

22. Costa Rocha, PA, Coelho De Sousa, R, Freitas De Andrade, C, Vieira Da Silva, ME: Comparison of seven numerical methods for determining Weibull parameters for wind energy generation in the northeast of Brazil. Applied Energy **89**, 395–400 (2012)

23. Chang, TP: Performance comparison of six numerical methods in estimating Weibull parameters for wind energy application. Applied Energy **88**, 272–282 (2011)

24. Mertens, SM, van Kuik, van Bussel, G: Performance of an H-Darrieus in the skewed flow on a roof. J. Solar Energy Eng. **125**, 433–440 (2003)

25. Li, Z, Boyle, F, Reynolds, A: Domestic application of micro wind turbines in Ireland: investigation of their economic viability. Renew Energy **41**, 64–74 (2011)

26. Patania, F, Gagliano, A, Nocera, F, Galesi, A: The noise pollution in nature protected area of the Pergusa Lake. Int. J. Design Nature Ecodynamics **6**, 52–67 (2011)

27. Tina, G, Gagliano, S, Raiti, S: Hybrid solar/wind power system probabilistic modelling for long-term performance assessment. Solar Energy **80**, 578–588 (2006)

28. Lopes, AMG: Windstation a software for the simulation of atmospheric flows over complex topography. Environ. Model Software **18**, 81–96 (2003)

29. Araújo, AM, Arraes De Alencar Valença, D, Asibor, AI, Carvalho Rosas, PA: An approach to simulate wind fields around an urban environment for wind energy application. Environ. Fluid Mech. **13**, 33–50 (2013)

30. Patania, F, Gagliano, A, Nocera, F, Galesi, A, D'Amico, A: An applied research to forecast the trend of air pollution in particular geometries of streets: the real case of urban canyon. WIT Transactions Ecology Environ. **86**, 33–44 (2006)

31. Li, X-X, Liu, C-H, Leunga, DYC, Lam, KM: Recent progress in CFD modelling of wind field and pollutant transport in street canyons. Atmos. Environ. **40**, 5640–5658 (2006)

32. Yoshie, R, Mochida, A, Tominaga, Y, Kataoka, H, Yoshikawa, M: Cross comparisons of CFD prediction for wind environment at pedestrian level around buildings. Part 1: comparison of results for flow-field around a high-rise building located in surrounding city blocks. In: 6th Asia-Pacific Conference on Wind Engineering. Seoul (2005)

33. EERE: Virtualwind. http://apps1.eere.energy.gov/buildings/tools_directory/software.cfm?ID=579/pagename=alpha_list_sub?print. Accessed November 2013

34. Sagaut, P: Large Eddy Simulation for Incompressible Flows. Springer, Berlin (2006)

35. McLean, W: Poisson solvers. http://www.cs.northwestern.edu/~jet/Teach/2004_3spr_IBMR/poisson.pdf. Accessed July 2013

36. Ledo, L, Kosasih, PB, Cooper, P: Roof mounting site analysis for micro-wind turbines. Renew. Energy **36**(5), 1379–1391 (2011)

37. Blackmore, P: Siting Micro-Wind Turbines on House Roofs. IHS BRE Press, Watford (2008)

38. Rafailidis, S: Influence of building areal density and roof shape on the wind characteristics above a town. Bound. Lay. Meteorol. **85**(2), 255–271 (1997)

39. Abohela, I, Hamza, N, Dudek, S: Effect of roof shape on energy yield and positioning of roof mounted wind turbines. In: Proceedings of 12th Conference of International Building Performance Simulation Association, Sydney, 14–16 November 2011

40. Mertens, S: Wind energy in the built environment. Multi-Science Publishing Co. Ltd., Essex (2006)

41. Sáenz-Díez Muro, JC, Jiménez Macías, E, Blanco Barrero, JM, Pérez De La Parte, M, Blanco Fernández, J: Two-dimensional model of wind flow on buildings to optimize the implementation of mini wind turbines in urban spaces. In: ICREPQ'10, Granada, 23–25 March 2010

42. Paterson, DA, Apelt, CJ: Simulation of wind flow around three-dimensional buildings. Build. Environ. **24**, 39–50 (1989)

43. Yoshie, R, Mochida, A, Tominaga, Y, Kataoka, H, Harimoto, K, Nozu, T: Cooperative Project for CFD Prediction of Pedestrian Wind Environment in the Architectural Institute of Japan. J. Wind Eng. Ind. Aerod. **95**, 1551–1578 (2007)

44. Chew, PL: Constrained Delaunay triangulations. Algorithmica. **4**, 97–108 (1989)

45. ESRI: ArcGIS desktop tutorials. http://webhelp.esri.com/arcgisdesktop/9.3/index.cfm?TopicName=tutorials. Accessed 10 May 2013

46. EERE: Building Energy software tools directory. http://apps1.eere.energy.gov/buildings/tools_directory/software.cfm/ID=579/pagename_submenu=solar_climate_analysis/pagename_menu=other_applications/pagename=subjects. Accessed July 2013

47. NOABL: Wind speed database. http://www.decc.gov.uk/en/content/cms/meeting_energy/wind/windsp_databas/windsp_databas.aspx (accessed). Accessed July 2013

48. Agrawal, N, Gupta, VK, Gupta, A, Mittal, A: Comparison of codal values and experimental data pertaining to dynamic wind characteristics. J. Wind Eng. **9**(1), 33–53 (2012)

49. Plate, EJ: Methods of investigating urban wind fields-physical models. Atmos. Environ. **33**, 3981–3989 (1999)

50. Raciti, M, Castelli, A, Benini, E: Modeling, strategy and numerical validation of the turbulent flow over a two-dimensional flat roof. World Acad. Sci. Eng. Technol. **79**, 462–468 (2011)

51. President of Italian Republic: Legislative Decree 3 March 2011 N° 28. http://www.acs.enea.it/doc/dlgs_28-2011.pdf. Accessed 10 May 2013

52. Energy Saving Trust: Domestic small-scale wind information. http://www.est.org.uk/myhome/generating/types/wind/. Accessed 10 May 2013

53. Tutto green: Eolico domestico o minieolico: quali sono le offerte sul mercato? http://www.tuttogreen.it/eolico-domestico-o-minieolico-quali-sono-le-offerte-sul-mercato/. Accessed10 May 2013

54. IPCC: Carbon dioxide intensities of fuels and electricity for regions and countries. http://www.ipcc.ch/pdf/special-reports/sroc/Tables/t0305.pdf. Accessed 10 May 2013

55. Ruggieri, G: Consumi elettrici nel settore domestico. http://www.aspoitalia.it/attachments/220_Gianluca%20Ruggieri%20%20Consumi%20elettrici%20nel%20domestico.pdf. Accessed 10 May 2013

56. Autorità per l'Energia: Elettrica ed il Gas. I servizi di vendita. http://www.autorita.energia.it/it/consumatori/bollettatrasp_ele.htm. Accessed 10 May 2013

57. D'haeseleer, WD, Voorspools, KR: An analytical formula for the capacity credit of wind power. Renew. Energy **31**, 45–54 (2006)

58. Kelleher, J, Ringwood, JV: A computational tool for evaluating the economics of solar and wind microgeneration of electricity. Energy **4**, 401–409 (2009)